

## Migration behavior of single tungsten atoms and tungsten diatomic clusters on the tungsten (110) plane

T. T. Tsong and Rodrigo Casanova

*Physics Department, The Pennsylvania State University, University Park, Pennsylvania 16802*

(Received 21 April 1980)

Detailed atomic jumps in the single W atom and W diatomic-cluster migration on the W{110} plane have been studied using the field ion microscope. From the two-dimensional displacement distributions measured at 299 and 309 K, it is concluded that single W atoms migrate by discrete nearest-neighbor random atomic jumps along the  $\langle 111 \rangle$  surface channels. From 1265 observations, the diatomic clusters are found to migrate mainly through three elementary displacement steps. The steps can be produced by two atomic jumps of any of the two atoms along the  $\langle 111 \rangle$  surface channels with intermediate bonds in the  $[1\bar{1}0]$  and  $[001]$  directions. These two atomic jumps are found to be slightly correlated with a correlation factor of 0.10 at 299 K and of 0.23 at 309 K. An anisotropy factor of the two-dimensional migrations is defined and measured. The pair interaction of two W atoms on the W{110} plane is also derived from the rate of single atom jumps and the rates of occurrence of diatomic-cluster elementary displacement steps. The interaction energy at the equilibrium separation is  $-(0.285 \pm 0.018)$  eV, while at the saddle point of the atomic jumps it is  $-(0.270 \pm 0.018)$  eV.

### I. INTRODUCTION

Tungsten {110} plane is one of the best investigated surfaces. In early days when modern surface-cleaning techniques were not yet available, flash desorption was the only reliable method of cleaning surfaces. Tungsten, with one of the highest melting points in all elements, was especially popular since the cleanliness of a surface by flash desorption could be assured. With the advent of the field ion microscope (FIM), atomically clean and perfect surfaces of tungsten and other metals can easily be obtained by field evaporations.<sup>1</sup> Tungsten remains a popular material for FIM studies, especially for FIM single-atom studies, because of the reliability of tungsten tips. Also, the {110} plane remains most popular since the size of the plane is large as compared to other planes on a field-evaporated W tip surface. Tungsten {110} plane is also known to have a very low sticking coefficient for chemically reactive gases, thus the cleanliness of the surface can be maintained for a longer period of time than any other plane. This last point is especially important for single-atom experiments since contamination of a few or even an atom on a plane may cause the entire set of data to be unreliable. It is generally recognized that despite great progress in vacuum and surface-preparation techniques, truly clean, contamination-free, and defect-free macroscopic surfaces are rare. Field evaporation is still a reliable way of developing a clean and atomically perfect surface. Data derived with such surfaces, with the assurance of maintaining the cleanliness of the surfaces during experiments, should be most valuable for a basic understanding of atomic processes occurring on solid surfaces.

From the structure aspect, however, the W {110} plane is one of the more complicated planes to study since the symmetry of the atomic structure is low. Analysis of data often presents a real challenge. In this report, we will present a detailed study of the migration behaviors of single W atoms and W diatomic clusters on the W {110} plane. We will identify the elementary displacement steps of the diatomic-cluster migration<sup>2</sup> by measuring the two-dimensional displacement distributions and also by a probabilistic consideration. Mechanisms of diatomic-cluster migration based on two correlated single atomic jumps in various directions will be proposed, and will be compared with the experimental data. We will point out how the pair interaction of single atoms dictates the migration behavior of a diatomic cluster, and how information on the pair interaction can be derived from the observed frequencies of the various elementary displacement steps of the cluster. For this purpose, the two-dimensional displacement distribution function of a single W atom on the same plane at the same temperature will also be presented. The anisotropy of the migration of single atoms,<sup>3</sup> and evidence of that of diatomic clusters on this plane will be given and discussed. We will establish quantitatively that the single W atoms indeed migrate by nearest-neighbor discrete jumps along the  $\langle 111 \rangle$  surface channels as proposed earlier.<sup>3</sup>

### II. EXPERIMENTAL PROCEDURES

Detailed procedures of single-atom FIM experiments are well established and can be found elsewhere.<sup>4,5</sup> We take extreme care and elaborate procedures in achieving the best possible vacuum

condition of the FIM. The FIM, after being open to air for a specimen replacement, is baked for ~20 hours at 250°C. After a baking, all the components in the system are carefully degassed by either ion bombardment for several hours using helium field ions or by heatings. The system is then subjected to the same baking and degassing procedures again. This process is repeated several times. Thus usually a week is gone before an experimental measurement can be started. The system, after the elaborate vacuum processing procedures, is always  $\sim 2 \times 10^{-11}$  Torr, the x-ray limit of the gauge, even without any cooling and even when the system is valved off from the pumps. We use exclusively helium for imaging. Ultrapure helium is obtained by diffusion through a Vycor glass bulk at 350°C. The bulb has been subjected to degassing at ~500°C earlier. The system is equipped with a titanium sublimation pump which is degassed thoroughly during bakings and is cooled down to liquid-nitrogen temperature during an experiment.

Two methods were used for depositing adatoms on field-evaporated W surface planes.<sup>2</sup> The first method retained one or two W atoms on a plane by carefully field evaporating the rest of the atoms in the top surface layer. The second method used heating of a carefully degassed W coil as is generally being done. The first method involved no generation of heat in the system after the system was valved off, thus no generation of contaminating gas might occur during the experiment. This method was, however, quite difficult, because the last few atoms tend to field-evaporate all together no matter whether a dc or a pulsed voltage was used for the field evaporation. However, we did not detect any difference in the behavior of either single atoms or diatomic clusters obtained by either of the two deposition methods; thus both methods were used in our experiment.

For detecting and measuring displacements of single atoms and diatomic clusters, both a color-comparator technique<sup>1</sup> and an image-mapping technique<sup>2</sup> were used. The two techniques when used carefully gave comparable precision. The color-comparator technique had the advantage of direct visualization of the displacements and the cluster-orientation changes, but suffered from tediousness when great precision was desired.

As mentioned earlier, we used exclusively Vycor glass diffused helium for the FI (field ion) imaging. As soon as one or two atoms were retained or deposited on a well-developed W {110} plane, routine procedures of heatings and imagings followed. Imagings were done at 78-K cooling of the sample. Each heating period was 60 sec. The measurements were carried out at two temperatures:

299±5 K and 309±5 K. The ±5 K accuracy referred to the reproducibility of the absolute temperature, which was estimated from single-atom diffusion data in various runs with different tips, and therefore different temperature calibrations. The accuracy of the relative temperature was better than ±0.5 K. Thus the temperature difference of the measurement was  $\Delta T = 10 \pm 0.5$  K. The reason that we did not go to higher temperatures is that the data become very difficult to analyze because of the relatively complicated migration behavior of the diatomic cluster on this plane of relatively complicated atomic structure. Also, at higher temperatures, the exact displacements of a cluster are more difficult to determine. All the data reported in this paper were obtained from the same W tip with the same temperature calibration. The data were derived with either one W atom or one W diatomic cluster on a W {110} plane.

### III. RESULTS AND DISCUSSIONS

#### A. General behavior

Single tungsten atoms are known to make detectable migration on the W {110} plane around 300 K.<sup>4,5</sup> The diffusion parameters have been derived with one atom on a plane<sup>5</sup> to be  $E_d = 0.90 \pm 0.07$  eV;  $D_0 = 6.2 \times 10^{-3} \times (13)^{+1}$  cm<sup>2</sup>/sec. The plane boundary is reflective.<sup>4,5</sup> Above ~370 K, an occasional loss of the migrating atom can occur.<sup>5</sup>

When two tungsten atoms are deposited on a plane, they will combine into a closely-packed diatomic cluster upon encountering each other during the migration.<sup>5,7</sup> The atoms in a cluster can be marginally resolved if the tip radius is very small, for example, less than 150 Å. The bond direction is along one of the <111> directions. Thus a cluster on a plane can have two orientations, as can be seen in Fig. 1. The diatomic cluster is thermally more stable than the triatomic cluster.<sup>6</sup> Thus a triatomic cluster can migrate by "dissociation-recombination" process. For diatomic clusters, this process may also occur but is of less importance since the clusters are thermally stable up to about 380 K; at this temperature the migration of both W and W<sub>2</sub> is too rapid for deriving accurate diffusion parameters on the small FI emitter planes. The diatomic W cluster is found to migrate at a slightly higher temperature than single W atoms. The diffusion parameters have been derived<sup>6</sup> with one cluster on a plane to be  $E_d = 0.92 \pm 0.14$  eV;  $D_0 = 1.4 \times 10^{-3} \times (160)^{+1}$  cm<sup>2</sup>/sec. The large statistical errors come from the narrow temperature range of the measurement rather than from the true accuracy of determining the mean-square displacement at a certain tempera-

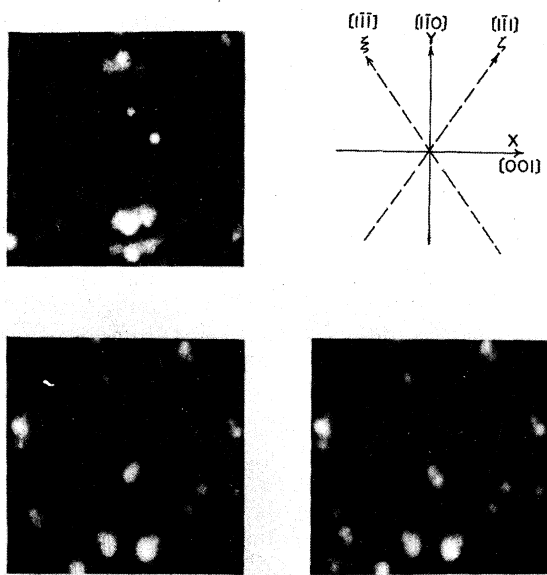


FIG. 1. Field ion images showing two W atoms on a W {110}, a W diatomic cluster oriented along the  $[111]$ , and one oriented along the  $[11\bar{1}]$ .

ture. The mobility of a diatomic cluster as indicated by the mean-square displacement is smaller than that of a single atom by a factor of about 8 around 300 K.

The exact sites of adsorption for single W atoms and W diatomic clusters are very difficult to pinpoint from field ion images since no atomic structure of the  $\{110\}$  plane can be directly seen in the FIM. For single atoms, four sites, as shown in Fig. 2, are of particular interest.<sup>3</sup> These sites are the apex site A, the bridge site B, the lattice site C, and the surface site D. Mappings of the locations of single W atoms on a plane indicates that W atoms sit most probably on lattice sites.<sup>8</sup> For diatomic clusters, evidence shows that their center of mass (c.m.) sits most probably on bridge sites, with individual atoms sitting in or close to lattice sites.<sup>2</sup> For our purpose here the precise site of adsorption is not critical to our discussion. As long as the energy barrier for jumps between two surface sites within a unit cell is small compared to jumps out of the unit cell, the two cases, lattice-site and surface-site adatom adsorption, make little difference. Our discussion will simply be based on lattice-site adsorption.

Since only one bond structure, the closely packed form, has been observed for the diatomic cluster, the migration mechanism cannot be directly visualized. From the frequent changes of cluster orientations relative to the substrate plane during a migration, and the small difference in the acti-

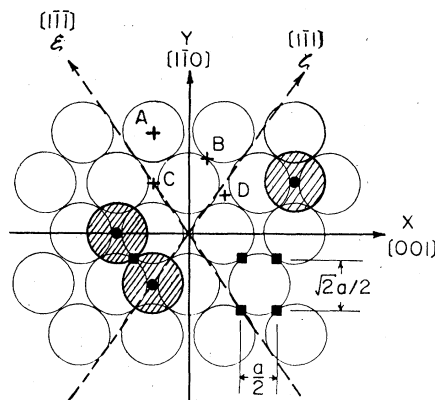


FIG. 2. Atomic structures of the W {110}. The sites as represented by A, B, C, and D correspond, respectively, to apex site, bridge site, lattice site, and surface site. Bridge sites form a rectangular lattice of unit cells  $a\hat{i}/2 \times \sqrt{2}a\hat{j}/2$ .

vation energy  $E_d$  for migration, it was speculated that the migration was accomplished by a bond stretching or by individual atomic jumps.<sup>6</sup> We will present here quantitative evidence supporting such an idea, and further propose the details of the atomic jumping process. For this purpose, we will first discuss the elementary displacement steps<sup>2</sup> in the diatomic cluster migration.

#### B. Identification of elementary displacement steps in diatomic-cluster migration

The elementary displacement steps will be defined as the displacements resulting from the smallest number of atomic jumps possible in producing a net displacement of the cluster. All other cluster displacements are therefore successive occurrences of more than one elementary displacement step. Recently we reported to have identified three elementary displacement steps.<sup>2</sup> We will present here a quantitatively more reliable amount of data (as many as 1265 heating periods at two heating temperatures) and a much more detailed analysis of the data. The analysis establishes without doubt the earlier identifications, and in addition finds out the rates of the single atomic jumps as well as a correlation factor of these jumps.

To identify the elementary displacement steps, the temperature must be low enough such that the probability of having two elementary displacement steps occurring successively within a heating period is very small. At 299 K, out of 761 heating periods of 60 sec each, a total of 204 displacements are observed. Each of them is carefully identified and classified using color-compara-

tor technique and is shown in Fig. 3. In this figure we also give symbolic representations of these observed displacements. In Table I, all 204 displacements are classified and listed. Because of the symmetry of the substrate surface structure, each displacement step of a diatomic cluster can occur in four directions, two from the bond direction of the cluster and two from the displacement direction. The possible bond directions are, of course,  $\zeta$  and  $\xi$  directions. The bond direction is represented by a thick bar in a symbol, whereas the "apparent" displacement direction of an atom is represented by an arrow. The word apparent here signifies two things. First, from field ion micrographs it is impossible to tell which of the two atoms has displaced. Second, one arrow does not necessarily mean that only one atomic jump has occurred. The symbols merely indicate the appearance of the cluster displacement. We have also performed the same kind of experiment at 309 K. Out of a total of 504 heating periods, 275 displacements are observed. The results are also listed in Table I. The 309-K data are obtained using mapping techniques, which is found to be as reliable as the color-comparator technique.

The field ion images and the superimposed images of all the displacement steps shown in Fig. 3 are available in color slides. Reproduction in publication is so difficult and often does injustice to the true quality of the images that we will not try to reproduce them here. However, field ion images and superimposed images leading to the identification of the displacement steps shown in Figs. 3(a)–3(c) have been published by us recently.<sup>2</sup>

In Fig. 4 we show two-dimensional c.m. displacement distributions obtained for the diatomic clus-

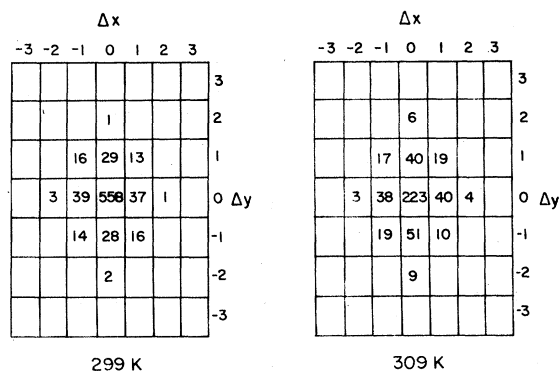


FIG. 4. Two-dimensional displacement distributions obtained from a tungsten diatomic cluster on a plane at 299 and 309 K. Each heating period is 60 sec.

ters at 299 and 309 K for heating periods of 60 sec each. The displacements here always refer to the c.m. Since the c.m. sits on a bridge site, the c.m. displacement vectors form a rectangular lattice of  $\frac{1}{2}a\hat{i} \times \frac{1}{2}\sqrt{2}a\hat{j}$  as shown in Fig. 2. The displacement distributions shown in Fig. 4 reflect this fact also. As displacements corresponding to those shown in Figs. 3(g) and 3(h) were identified at the last minute and their numbers were quite small, we have omitted listing them in the displacement distributions. This minor omission will not affect our analysis and conclusion.

To search for the mechanisms of migration of the diatomic cluster, we have to identify the elementary cluster displacement steps first. We have recently identified those displacements shown in Figs. 1(a)–1(c) to be elementary, based on a semiquantitative probability consideration.<sup>2</sup> We present here two methods of analysis, one based on the two-dimensional displacement distribution functions, and the other based on a detailed probability consideration. Since the displacement vectors of the cluster c.m. form a rectangular lattice of unit cells  $\frac{1}{2}a\hat{i} \times \frac{1}{2}\sqrt{2}a\hat{j}$ , the shortest possible displacements of the c.m. are  $\frac{1}{2}a\hat{i}$  and  $\frac{1}{2}\sqrt{2}a\hat{j}$ . Single cluster displacement steps leading to such displacements are necessarily elementary. Obviously the steps shown in Figs. 3(b) and 3(c) belong to this category. For brevity, they will be referred to as the  $\alpha$  and  $\beta$  steps, respectively. The question is whether some of the other displacements observed and shown in Fig. 3 are also elementary. For this purpose, we will simply, for the time being, assume that the  $\alpha$  and  $\beta$  steps are the only elementary displacement steps in the diatomic-cluster migration since all other displacements can be formed by combinations of the  $\alpha$  and  $\beta$  steps. We will calculate two-dimensional displacement distribution functions based on this

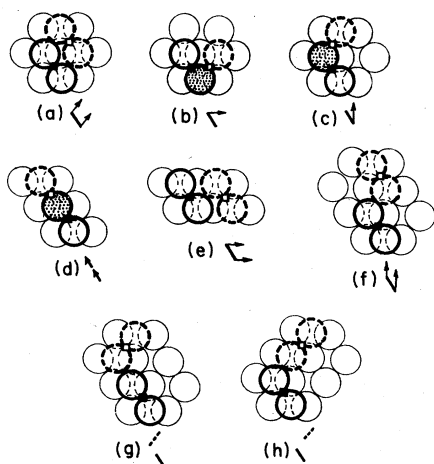
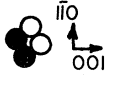


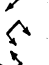
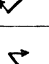
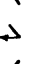


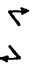
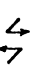
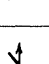
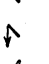

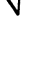
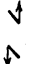
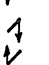
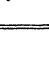




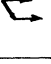



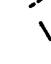


FIG. 3. Eight displacements observed at 299 K. Symbols of these displacements are also shown.

TABLE I. Frequencies of displacement steps observed in a total of 761 heating periods at 299 K and 504 heating periods at 309 K.

Displacement step observed	Symbol	299 K			309 K		
		Freq. obser.	Total No.	Average prob.	Freq. obser.	Total No.	Average prob.
		   	11			16	
		13	55	55/761	17	52	52/504
		15			11		
		16			8		
		   	22			24	
		17	76	76/761	14	78	78/504
		19			21		
		18			19		
		   	16			31	
		12	57	57/761	20	91	91/504
		13			18		
		16			22		
			4	0.47/761		13	1.17/504
			4	0.32/761		7	0.50/504
			3	0.36/761		15	0.68/504
			4	0.80/761		19	1.45/504
Unidentified large displacements			0			5	
% of change in bond orientation			68.2 %			68.0 %	

● Initial site

○ Final site

⊗ Initial and final site

assumption, and then compare these theoretical displacement functions with the experimental ones.

The one-dimensional displacement distribution function for nearest-neighbor discrete random walk is well known and is given by<sup>8,9</sup>

$$W(x) = \exp(-\bar{N}) I_x(\bar{N}), \quad (1)$$

where

$$I_x(\bar{N}) = \sum_{k=0}^{\infty} \left( \frac{\bar{N}}{2} \right)^{(x+2k)} / k! (x+k)! \quad (2)$$

is the modified Bessel function of the first kind.

$W(x)$  represents the probability of reaching  $x$  when the average number of jumps occurring within a heating period is  $\bar{N}$ . On a rectangular lattice the two-dimensional displacement distribution function is then given by

$$W(x, y) = \exp[-(\bar{N}_\alpha + \bar{N}_\beta)] I_x(\bar{N}_\alpha) I_y(\bar{N}_\beta), \quad (3)$$

where  $\bar{N}_\alpha$  and  $\bar{N}_\beta$  are, respectively, the average number of  $\alpha$  and  $\beta$  steps which occurred within a heating period. In principle,  $\bar{N}_\alpha$  and  $\bar{N}_\beta$  can be obtained from a least-squares fit of the experimental displacement distribution if it is certain

that the  $\alpha$  and  $\beta$  steps are the only elementary displacement steps in the diatomic-cluster migration. Since this is not the case, as will be clear from further discussions, we will do it slightly differently. At low temperatures when the probability of having two elementary displacement steps occur within a heating period is very small, the displacements in  $x$  and  $y$  directions act nearly independently. Thus  $\bar{N}_\alpha \approx \langle (\Delta x)^2 \rangle$ , and  $\bar{N}_\beta \approx \langle (\Delta y)^2 \rangle$ . Using the data shown in Fig. 4 for  $\Delta y = 0$  and  $\Delta x = 0$ , we obtain the following values:  $\bar{N}_x \approx 0.1206$ ,  $\bar{N}_y \approx 0.0905$  at 299 K, and  $\bar{N}_x \approx 0.211$ ,  $\bar{N}_y \approx 0.300$  at 309 K. In Fig. 5 we show both the symmetrically averaged and normalized experimental displacement distribution functions (DDF) and the calculated DDF at 299 and 309 K. The normalized experimental DDF are obtained by taking the average of values at  $+\Delta x$  and  $-\Delta x$  and values at  $+\Delta y$  and  $-\Delta y$ . We do not average over those values with  $\pm \Delta x = \pm \Delta y$  for the reason that  $\bar{N}_\alpha$  seems to differ significantly from  $\bar{N}_\beta$  as can be seen from Table I. This point will be discussed later.

As can be seen from these diagrams, the experimental and calculated frequencies agree reasonably well for all sites except at four sites corresponding to  $\Delta x = \pm 1$  and  $\Delta y = \pm 1$ . For these four sites, the experimentally determined frequency is larger than the calculated frequency by a factor of 700% at 299 K and of 333% at 309 K. The much larger experimental values indicate that the  $\alpha$  and  $\beta$  steps are not all the elementary displacement steps in the diatomic-cluster migration. The

displacements corresponding to  $\Delta x = \pm 1$  and  $\Delta y = \pm 1$ , or  $\Delta \vec{r} = \pm \frac{1}{2} a \hat{i} \pm \frac{1}{2} \sqrt{2} a \hat{j}$ , can of course be achieved by a single step of the observed displacement shown in Fig. 3(a). We must therefore conclude that the observed displacement step shown in Fig. 3(a) is also elementary; such a displacement step will be referred to as the  $\gamma$  step. The corresponding average number of occurrences within a heating period will be represented by  $\bar{N}_\gamma$ .

The same conclusion can also be reached by a more straightforward consideration of the rates of occurrence of the elementary displacement steps at a given temperature. They will be represented respectively by  $k_\alpha$ ,  $k_\beta$ , and  $k_\gamma$ . We distinguish the rates of occurrence from the rates observed since a successive occurrence of, for example, an  $\alpha$  and a  $\beta$  step will result in the observation of a  $\gamma$  step, thus indistinguishable from the true occurrence of a  $\gamma$  step. We want to find the probability  $P_{i,j}$  of occurrence of two different elementary steps, for example,  $i$  and  $j$  in that sequence within a heating period  $\tau$ .  $i$  and  $j$  are indices representing either  $\alpha$ ,  $\beta$ , or  $\gamma$ .  $P_{i,j}$  can be found by taking the time average of the probability that within  $t$  the  $i$  step occurs once, and within the rest of the time  $(\tau - t)$  the  $j$  step occurs exactly once:

$$P_{i,j} = \frac{1}{\tau} \int_0^\tau P_i(1,t) P_j(1,\tau-t) dt. \quad (4)$$

$P_i(1,t)$  and  $P_j(1,\tau-t)$  are given by Poisson's distribution to be

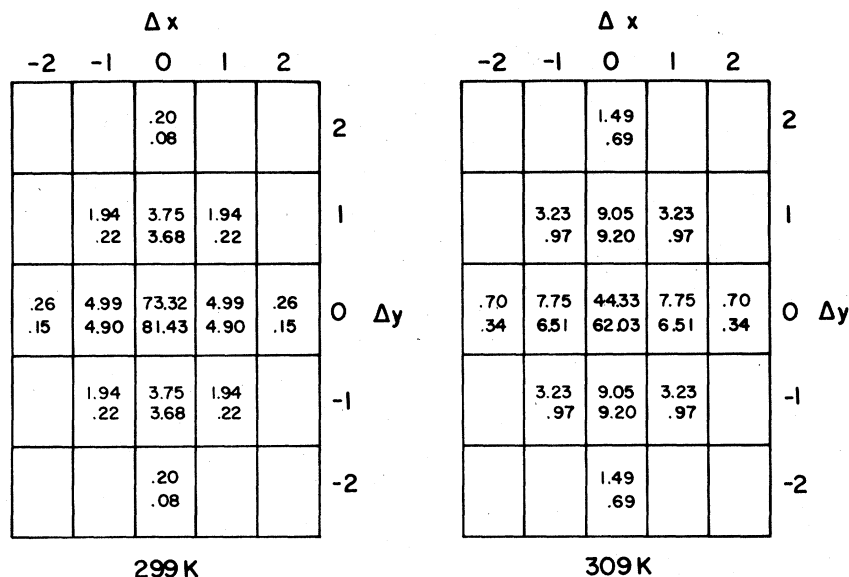


FIG. 5. Experimental and calculated two-dimensional displacement distributions at 299 and 309 K for diatomic clusters. Experimental values are listed above the calculated values. Calculation is based on the assumption that only the  $\alpha$  and  $\beta$  steps occur.

$$P_i(1, t) = k_i t e^{-k_i t}, \quad (5)$$

$$P_j(i, \tau - t) = k_j(\tau - t) e^{-k_j(\tau - t)}. \quad (6)$$

If  $k_i \approx k_j$ , and  $k_i \tau < 1$  and  $k_j \tau < 1$ , one has

$$P_{i,j} = \frac{1}{6}(k_i \tau)(k_j \tau) e^{-k_j \tau}. \quad (7)$$

$k_i \tau$  is, of course, the average number of  $i$  steps which occurred within  $\tau$ . If  $k_i \tau < 1$  it is also the average probability of occurrence of an  $i$  step within  $\tau$ . Provided that  $k_i \tau \ll 1$  and  $k_j \tau \ll 1$ , one has

$$P_{i,j} \approx \frac{1}{6}(k_i \tau)(k_j \tau). \quad (8)$$

Similarly, the probability of occurrence of three different elementary steps, for example,  $i$  followed by  $j$  followed by  $k$  within a heating period  $\tau$  can be found by

$$P_{i,j,k} = \frac{1}{\tau} \int_0^\tau dt \int_0^{\tau-t} dt' [P_i(1, t) P_j(1, t') \times P_k(1, \tau - t - t')]. \quad (9)$$

under the condition that  $k_i \tau \approx k_j \tau \approx k_k \tau \ll 1$ , the equation reduces to

$$P_{i,j,k} \approx (k_i \tau)(k_j \tau)(k_k \tau)/120. \quad (10)$$

The probability of occurrence of two identical elementary steps in  $\tau$  is simply given by Poisson's distribution to be

$$P_{i,i} = \frac{1}{2}(k_i \tau)^2 e^{-k_i \tau}. \quad (11)$$

We are now ready to show again that the  $\gamma$  step is not a successive occurrence of an  $\alpha$  and a  $\beta$  step. Let us assume that the initial orientation of a diatomic cluster is along the  $\xi$  axis. A successive occurrence of an  $\alpha$  and a  $\beta$  step, either in  $\alpha, \beta$ , or  $\beta, \alpha$  sequence will result in a displacement of the cluster c.m. to  $\Delta x = \Delta y = 1$  site without an orientation change, thus will produce a  $\gamma$  step. This probability is

$$p \approx 2\frac{1}{6}(k_\alpha \tau)(k_\beta \tau). \quad (12)$$

From Fig. 4, we can find that at 299 K the average value of  $k_\alpha \tau \approx 38/761$ , and  $k_\beta \tau \approx 28.5/761$ . Thus  $p \approx 0.47/761$ . The experimental value, averaged over four sites at  $\Delta x = \pm 1$  and  $\Delta y = \pm 1$  is  $14.75/761$ ; the experimental value is larger than the calculated value by a factor of 31.4. At 309 K,  $k_\alpha \tau \approx 39/504$  and  $k_\beta \tau \approx 45.5/504$ . Thus  $p \approx 1.28/504$ . The average experimental value is  $16.3/504$ ; this is larger than the calculated value by a factor of 12.7. Thus the observed displacements  $\pm \frac{1}{2} a \hat{i}$  or  $\pm \frac{1}{2} \sqrt{2} a \hat{j}$  cannot be due to successive occurrences of an  $\alpha$  step and a  $\beta$  step. The displacements are therefore clearly established to be due to the occurrences of  $\gamma$  elementary displacement steps.

The question remains whether some of the displacements observed and shown in Fig. 3 are also

elementary. For this purpose, the displacements formed by two of the three elementary steps are listed in Table II, and the expected probabilities of occurrence of these displacements are listed in Table III. Using the experimental values listed in Table I for  $\alpha$ ,  $\beta$ , and  $\gamma$  steps, and the expected probability expression listed in Table III, the expected probabilities of other observed displacements are calculated and listed also in Table I.

By comparing these calculated values with the observed values one must conclude that most of these observed displacements at 299 K are very probably elementary also. However, the frequencies of observing these displacements are small and our analysis is not exact, thus no definite conclusion can be drawn at this moment. To be able to establish quantitatively any of these displacements as elementary displacement steps, the amount of data needed will be formidably large with the present data-collecting method. Since these displacements occur rarely as compared to  $\alpha$ ,  $\beta$ , and  $\gamma$  displacement steps, even if some of them are elementary, they are less important than the three identified ones. Thus we may neglect considering them as elementary without introducing much error. However, a definitive identification will facilitate derivation of the pair interaction at large distances.


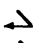
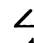




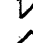
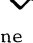
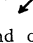
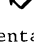
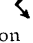

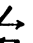

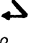


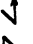

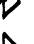
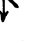

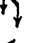



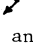









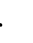

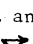
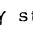







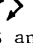
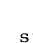










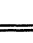
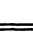
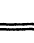



One can now calculate the two-dimensional displacement distribution function for the diatomic clusters based on the three identified elementary displacement steps which should approximate well the experimental distribution.

A method of calculating the two-dimensional displacement distribution function for the diatomic clusters based on the three identified elementary displacement steps is presented in the Appendix, where we show how the rates of occurrence of these elementary steps can be found by best fits of the calculated two-dimensional displacement distributions to the experimental distributions. From the rates derived one can then calculate a correlation factor for the atomic jumps as will be further discussed in Sec. III D.

#### C. Anisotropy in the migration of single atoms and diatomic clusters on the W {110} plane

Anisotropy of single-atom diffusion on the W {110} was found the first time migration of adatoms on a plane was studied with only one atom on the plane; thus mapping of many successive displacements of the same atom became possible.<sup>5</sup> It was found that an Re atom on a W {110} gave a mean-square displacement in the  $[1\bar{1}0]$  direction larger than that in the  $[001]$  direction by a factor of 2.09. From this observation it was concluded that the

TABLE II. Displacements formed by one or two elementary displacement steps.

Single step					Displacement	Orientation change
$\alpha$ step					$\pm a\hat{i}/2$	$(-1)$
$\beta$ step					$\pm 2a\hat{j}/2$	$(-1)$
$\gamma$ step					$\pm a\hat{i}/2 \pm 2a\hat{j}/2$	$(+1)$
Two steps: Only one bond orientation is considered.						
1. Two $\alpha$ steps						
(a)		+		=		(b)
(c)		+		=		(d)
2. Two $\beta$ steps						
(a)		+		=		(b)
(c)		+		=		(d)
3. Two $\gamma$ steps						
(a)		+		=		(b)
(c)		+		=		(d)
4. One $\alpha$ and one $\beta$ step						
(a)		+		=		(b)
(c)		+		=		(d)
(e)		+		=		(f)
(g)		+		=		(h)
5. One $\alpha$ and one $\gamma$ step						
(a)		+		=		(b)
(c)		+		=		(d)
(e)		+		=		(f)
(g)		+		=		(h)
6. One $\beta$ and one $\gamma$ step						
(a)		+		=		(b)
(c)		+		=		(d)
(e)		+		=		(f)
(g)		+		=		(h)

Re atom migrated by jumps along the  $\langle 111 \rangle$  surface channels of the plane. We will present here quantitative data supporting such a mechanism of single-atom migration. We will also give quantitative data showing a similar anisotropy in the diatomic-cluster migration on this plane.

Consider first the single-atom migration. Let us assume that a W atom on the W  $\{110\}$  will indeed migrate on the plane by discrete nearest-neighbor jumps along the  $[1\bar{1}1]$  and the  $[11\bar{1}]$  surface channel directions. We will calculate both the ratio of  $\langle (\Delta y)^2 \rangle / \langle (\Delta x)^2 \rangle$  and the two-dimensional displacement distribution functions based on such assumption. By showing excellent agreement of our experimental data with the calculated distribution, the validity of the assumption will be established. Let us consider here how the mean-square displacement along the  $x$  and  $y$  directions

are related to those along the  $\zeta$  and  $\xi$  directions. From Fig. 2 it is clear that

$$\begin{aligned} x &= (\zeta - \xi) \cos \alpha, \\ y &= (\zeta + \xi) \sin \alpha, \end{aligned} \quad (13)$$

where

$$\alpha = \tan^{-1} \sqrt{2} = 54.74^\circ.$$

Thus

$$\langle (\Delta x)^2 \rangle = [\langle (\Delta \zeta)^2 \rangle + \langle (\Delta \xi)^2 \rangle] \cos^2 \alpha, \quad (14)$$

$$\langle (\Delta y)^2 \rangle = [\langle (\Delta \zeta)^2 \rangle + \langle (\Delta \xi)^2 \rangle] \sin^2 \alpha. \quad (15)$$


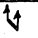




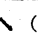



We therefore have

$$R \equiv \langle (\Delta y)^2 \rangle / \langle (\Delta x)^2 \rangle = \tan^2 \alpha = 2. \quad (16)$$

The factor  $R$  indicates the degree of anisotropy of



TABLE III. Probability of occurrence of a displacement by two elementary displacement steps.

Process	Prob. of occurrence	Remarks
	$p_{\alpha}^2/(6 \times 4 \times 4)$	$p_{\alpha}/4$ is the prob. of occur. of one particular $\alpha$ step.
Any one of the four similar proc.	$p_{\alpha}^2/24$	
	$p_{\beta}^2/(6 \times 4 \times 4)$	
Any one of the four similar proc.	$p_{\beta}^2/24$	
	$p_{\gamma}^2/(2 \times 4 \times 4)$	Occur. of two identical proc.
Any one of the four similar proc.	$p_{\gamma}^2/8$	
	$2p_{\alpha}p_{\beta}/(6 \times 4 \times 4)$	2 comes from the fact that two combinations will give the same displacement
Any one of the four similar proc.	$p_{\alpha}p_{\beta}/12$	
	$p_{\alpha}p_{\gamma}/(6 \times 4 \times 4)$	
	$p_{\alpha}p_{\gamma}/(6 \times 4 \times 4)$	
Any one of the 16 similar proc.	$(p_{\alpha}p_{\gamma} + p_{\beta}p_{\gamma})/12$	
	$2(p_{\alpha}^2/16 + p_{\beta}^2/16 + p_{\gamma}^2/16)/6$	
Any one of the two orientations	$(p_{\alpha}^2 + p_{\beta}^2 + p_{\gamma}^2)/24$	
	$2p_{\alpha}p_{\beta}/(6 \times 4 \times 4)$	2 comes from the fact that two combinations will give the same displacement
Any one of the four similar proc.	$p_{\alpha}p_{\beta}/12$	
	$2p_{\alpha}p_{\gamma}/(6 \times 4 \times 4)$	2 comes from the same reason as above
Any one of the four similar proc.	$p_{\alpha}p_{\gamma}/12$	
	$2p_{\beta}p_{\gamma}/(6 \times 4 \times 4)$	
Any one of the four similar proc.	$p_{\beta}p_{\gamma}/12$	
$p_{\alpha}$ , $p_{\beta}$ , and $p_{\gamma}$ are, respectively, the probabilities of occurrence of $\alpha$ , $\beta$ , and $\gamma$ elementary steps.		

the two-dimensional migration and will be referred to as an anisotropy factor. And

$$\begin{aligned} \langle (\Delta r)^2 \rangle &= [\langle (\Delta x)^2 \rangle + \langle (\Delta y)^2 \rangle] = \bar{N} l^2 \\ &= [\langle (\Delta \xi)^2 \rangle + \langle (\Delta \zeta)^2 \rangle] = (\bar{N}_{\xi} + \bar{N}_{\zeta}) l^2, \end{aligned} \quad (17)$$

where  $\bar{N}$ ,  $\bar{N}_{\xi}$ , and  $\bar{N}_{\zeta}$  are, respectively, the average total number of atomic jumps, the average number of jumps in  $\xi$  direction, and the average number of jumps in  $\zeta$  direction in a heating period  $\tau$ . It is obvious that

$$\bar{N} = \bar{N}_{\xi} + \bar{N}_{\zeta} \quad (18)$$

as it should. The two-dimensional displacement distribution functions can be calculated according to

$$W(\zeta, \xi) = \exp[-(\bar{N}_{\xi} + \bar{N}_{\zeta})] I_{\xi}(\bar{N}_{\xi}) I_{\zeta}(\bar{N}_{\zeta}). \quad (19)$$

From the symmetry of the plane, however, we should have  $\bar{N}_{\xi} = \bar{N}_{\zeta} = \bar{N}/2$  for single atoms.

In Figs. 6(a) and 6(b), the two-dimensional displacement distributions measured at 299 and 309 K for single W atoms are shown. In Table IV and Fig. 7 the same distributions are shown but they are projected onto the  $x$  axis and  $y$  axis. As can be seen from the Table, the anisotropy factor  $R$  is found to be 1.88 from the 299-K data, and to be 2.14 from the 309-K data. The average is 2.01, within 0.5% of the expected value of 2.

It should be pointed out here that the same value of  $R=2$  can also be expected if instead the atom

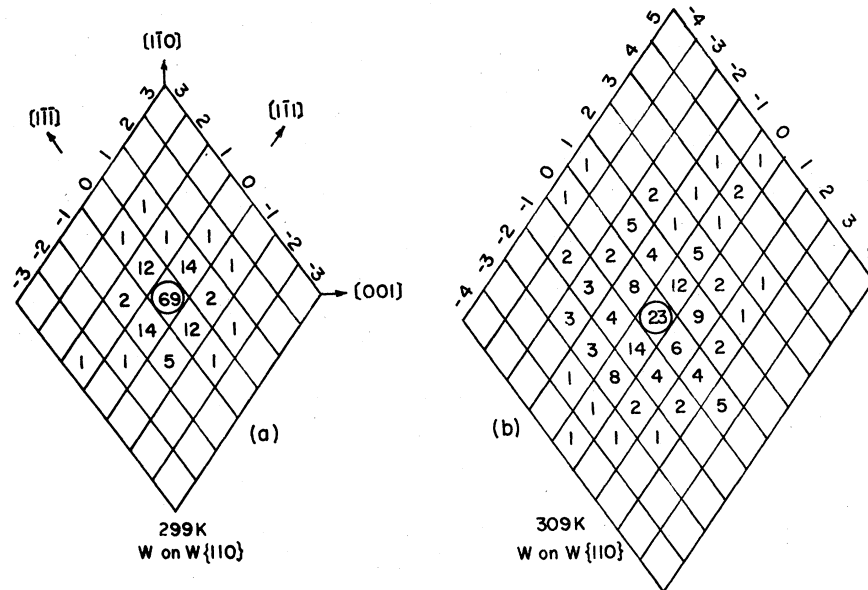


FIG. 6. Two-dimensional displacement distribution measured for single W atoms on the W {110} plane at 299 and 309 K. Each heating period is 60 sec.

jumps along the  $[1\bar{1}0]$  and the  $[001]$  directions over the apex of surface atoms. Thus the fact that  $R$  is measured to be 2.01 is only consistent with our assumption of atomic jumps along the  $\langle 111 \rangle$  surface channels, but does not exclude the possibility of jumps along the  $[1\bar{1}0]$  and  $[001]$  directions. However, from the two-dimensional DDF, one can exclude the latter mechanism as will be clear from further discussions.

Let us consider this point semiquantitatively.

If atomic jumps are dominantly in the  $[1\bar{1}0]$  and  $[001]$  directions, then the frequencies of observation in sites represented by  $\Delta\xi = \pm 1$  and by  $\Delta\xi = \pm 1$  in the DDF should be much larger than those in sites  $\Delta\xi = 0$ ,  $\Delta\xi = \pm 1$ ; and  $\Delta\xi = \pm 1$ ,  $\Delta\xi = 0$ . The fact that this is not the case, as can be seen from Fig. 6, shows that the atomic jumps cannot be dominantly in the  $[1\bar{1}0]$  and  $[001]$  directions. We will further show that these jumps most probably do not occur at all at low temperatures.

TABLE IV. Projected displacement distribution: W on W {110}.

$\Delta x$ (in $a/2$ )	Freq.	% Freq.	$\Delta y$ (in $\sqrt{2}a/2$ )	Freq.	% Freq.
299 K, 60 sec, 138 periods					
0	75	54.3	0	73	52.9
$\pm 1$	53	38.4	$\pm 1$	54	39.1
$\pm 2$	8	6.0	$\pm 2$	10	7.2
$\pm 3$	1	0.7	$\pm 3$	1	0.7
$\pm 4$	1	0.7	$\pm 4$	0	0
$\langle (\Delta x)^2 \rangle = 0.1993a^2$ , $\langle (\Delta y)^2 \rangle = 0.3732a^2$ , $R = 1.88$					
309 K, 60 sec, 150 periods					
0	34	22.7	0	40	26.7
$\pm 1$	50	33.3	$\pm 1$	51	34.0
$\pm 2$	35	23.3	$\pm 2$	31	20.7
$\pm 3$	16	10.7	$\pm 3$	15	10.0
$\pm 4$	14	9.3	$\pm 4$	10	6.7
$\pm 5$	1	0.7	$\pm 5$	1	0.7
$\pm 6$	0	0	$\pm 6$	0	0
			$\pm 7$	0	0
			$\pm 8$	2	1.3
$\langle (\Delta x)^2 \rangle = 0.9717a^2$ , $\langle (\Delta y)^2 \rangle = 2.0767a^2$ , $R = 2.14$					

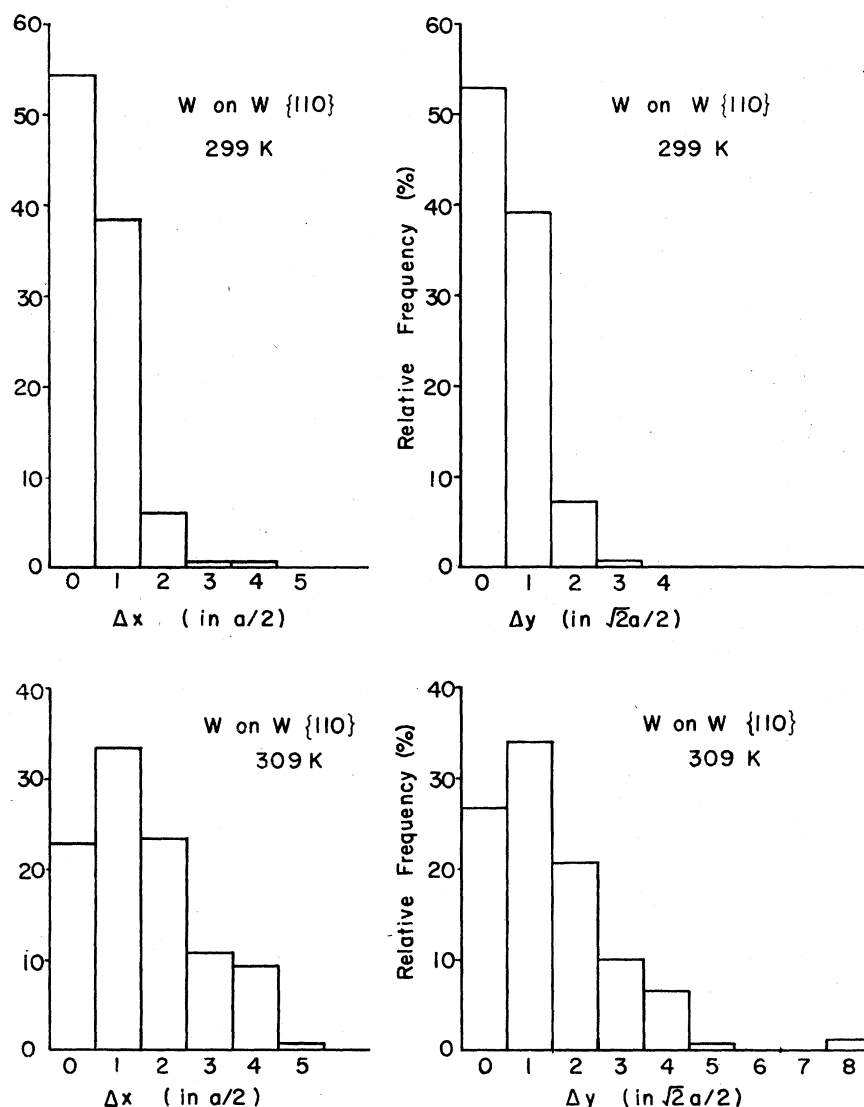


FIG. 7. Projected one-dimensional displacement distributions for single W atoms.

From Table IV,  $\langle(\Delta r)^2\rangle$  is found to be  $0.5725a^2 = 0.7631l^2$  at 299 K where  $l$  is the nearest-neighbor distance and  $a$  is the lattice constant. Thus  $\bar{N}_c = \bar{N}_t = 0.3815$ . Similarly, at 309 K,  $\bar{N}_c = \bar{N}_t = 2.032$ . Using these values, normalized two-dimensional DDF are calculated and are listed in Table V in parenthesis. The experimental DDF, derived from Fig. 6 by a proper normalization and symmetry averaging, are also listed in Table V. As can be seen, at 299 K all the experimental values agree remarkably well with the calculated values, all within the statistical fluctuations. At 309 K, the agreement is still very good although for sites  $\Delta\zeta = \Delta\xi = 0$  and  $\Delta\zeta = \Delta\xi = \pm 1$ , experimental values deviate very slightly beyond the expected

statistical fluctuations. Whether this deviation is significant or not is not clear. Further study is needed at higher temperatures. We thus conclude that at low temperatures, single-atom migration is achieved exclusively by nearest-neighbor jumps along the  $\langle 111 \rangle$  surface channels. At higher temperatures, the jumps may extend beyond the nearest-neighbor sites.<sup>9,10</sup> Also, jumps along the  $[1\bar{1}0]$  and  $[001]$  may not be completely ignored.

The diatomic-cluster migration also shows strong anisotropy. If the cluster migration is achieved exclusively by the  $\alpha$ ,  $\beta$ , and  $\gamma$  elementary displacement steps, then

$$\langle(\Delta x)^2\rangle = (n_\alpha + n_\gamma)a^2/4, \quad (20)$$

TABLE V. Two-dimensional displacement distribution function: W on W {110}; heating periods were 60 sec each; experimental values were averaged.

$\Delta\xi$	$\Delta\zeta$	0	$\pm 1$	$\pm 2$	$\pm 3$	$\pm 4$
299 K, 138 heating periods						
0		50.00 $\pm$ 6.02 (50.11)	9.42 $\pm$ 1.31 (9.39)	0.72 $\pm$ 0.18 (0.89)	0 (0.06)	0 (0.00)
$\pm 1$		9.42 $\pm$ 1.31 (9.39)	1.81 $\pm$ 0.57 (1.76)	0.36 $\pm$ 0.21 (0.17)	0.12 $\pm$ 0.12 (0.01)	0 (0.00)
$\pm 2$		0.72 $\pm$ 0.18 (0.89)	0.36 $\pm$ 0.21 (0.17)	0 (0.02)	0 (0.00)	0 (0.00)
$\pm 3$		0 (0.06)	0.12 $\pm$ 0.12 (0.01)	0 (0.00)	0 (0.00)	0 (0.00)
$\pm 4$		0 (0.00)	0 (0.00)	0 (0.00)	0 (0.00)	0 (0.00)
309 K, 150 heating periods						
0		15.33 $\pm$ 3.20 (9.34)	6.67 $\pm$ 1.05 (6.56)	3.17 $\pm$ 0.73 (2.88)	1.17 $\pm$ 0.44 (0.90)	0.67 $\pm$ 0.33 (0.22)
$\pm 1$		6.67 $\pm$ 1.05 (6.56)	3.50 $\pm$ 0.76 (4.61)	2.22 $\pm$ 0.50 (2.02)	0.56 $\pm$ 0.25 (0.63)	0.22 $\pm$ 0.16 (0.15)
$\pm 2$		3.17 $\pm$ 0.73 (2.88)	2.22 $\pm$ 0.50 (2.02)	1.17 $\pm$ 0.44 (0.89)	0.11 $\pm$ 0.11 (0.28)	0 (0.07)
$\pm 3$		1.17 $\pm$ 0.44 (0.90)	0.56 $\pm$ 0.25 (0.63)	0.11 $\pm$ 0.11 (0.28)	0 (0.09)	0 (0.02)
$\pm 4$		0.67 $\pm$ 0.33 (0.22)	0.22 $\pm$ 0.16 (0.15)	0 (0.07)	0 (0.02)	0 (0.01)

$$\langle(\Delta y)^2\rangle = (n_\beta + n_\gamma)a^2/2, \quad (21)$$

and

$$\langle(\Delta r)^2\rangle = \left(\frac{n_\alpha}{4} + \frac{n_\beta}{2} + \frac{3}{4}n_\gamma\right)a^2. \quad (22)$$

In the equations,  $n_\alpha$ ,  $n_\beta$ , and  $n_\gamma$  represent, respectively, the average number of occurrences, of  $\alpha$ ,  $\beta$ , and  $\gamma$  steps within a heating period. The anisotropic factor  $R$  of the cluster migration as defined in Eq. (16) is given by

$$R = 2 \frac{(n_\beta + n_\gamma)}{(n_\alpha + n_\gamma)} = 2 \left( \frac{1}{k_\beta} + \frac{1}{k_\gamma} \right) / \left( \frac{1}{k_\alpha} + \frac{1}{k_\gamma} \right), \quad (23)$$

where  $k_\alpha$ ,  $k_\beta$ , and  $k_\gamma$  represent, respectively, the rates of occurrence of  $\alpha$ ,  $\beta$ , and  $\gamma$  steps. If  $k_\alpha = k_\beta$ , then  $R=2$  is obtained as in the single-atom migration.

The experimental data, given in the form of two-dimensional DDF, shown in Fig. 4 are rearranged by projecting them along  $x$  and  $y$  axes and are tabulated in Table VI. From the data, it can be easily calculated that at 299 K,  $R=1.70$ , and at 309 K,  $R=2.53$ . Although the value of  $R=2.12$ , obtained by averaging experimental values at the two temperatures, is not too far off from 2, the observed

temperature dependence of  $R$  in diatomic cluster seems significant. At 299 K, we observe more  $\alpha$  steps than  $\beta$  steps in every run of our experiment. The situation is reversed at 309 K. Unfortunately, to settle this question quantitatively we will need a formidable amount of data, which is tedious to collect with the present technique of resistive heating, but may become practical using pulsed-laser heating of sample tips as has been reported recently.<sup>11</sup>

It should be pointed out here that the orientation of a diatomic cluster is not arbitrary on a site since the three elementary cluster-migration steps have a definitive relationship between a displacement and the orientation change. When two atoms combine at a certain site (referring to the c.m.), the bond direction formed then determines the orientation of the cluster at any given site on the plane. This can be understood as follows: An  $\alpha$  step will produce a c.m. displacement of  $\pm \frac{1}{2}a\hat{i}$  and will be accompanied by a bond-orientation change. A  $\beta$  step will produce a c.m. displacement of  $\pm \frac{1}{2}\sqrt{2}a\hat{j}$  and will be accompanied by an orientation change also. A  $\gamma$  step will produce a c.m. displacement of  $\pm \frac{1}{2}a\hat{i} \pm \frac{1}{2}\sqrt{2}a\hat{j}$  without changing a bond orientation. Thus an orientation operator

TABLE VI. Projected displacement distribution.  $W_2$  on W {110}.

$\Delta x$ (in $a/2$ )	Freq.	% Freq.	$\Delta y$ (in $\sqrt{2}a/2$ )	Freq.	% Freq.
299 K					
0	618	81.64	0	638	84.28
$\pm 1$	135	17.83	$\pm 1$	116	15.32
$\pm 2$	4	0.53	$\pm 2$	3	0.40
$\pm 3$	0	0	$\pm 3$	0	0
$\langle(\Delta x)^2\rangle = 0.0499a^2$ , $\langle(\Delta y)^2\rangle = 0.0845a^2$ , $R = 1.70$					
309 K					
0	329	68.68	0	308	64.30
$\pm 1$	143	29.85	$\pm 1$	156	32.57
$\pm 2$	7	1.46	$\pm 2$	15	3.13
$\pm 3$	0	0	$\pm 3$	0	0
$\langle(\Delta x)^2\rangle = 0.0892a^2$ , $\langle(\Delta y)^2\rangle = 0.2255a^2$ , $R = 2.53$					

can be used to indicate the orientation of the cluster after a displacement,

$$0 = (\pm 1) \times (-1)^{(\Delta x + \Delta y)}. \quad (24)$$

The first factor indicates the initial orientation of the cluster with +1 representing the bond direction along the  $\zeta$  axis, and -1 representing the bond direction along the  $\xi$  axis.  $\Delta x$  and  $\Delta y$  represent, respectively, the net displacements in units of  $\frac{1}{2}a$  in the  $x$  direction and  $\frac{1}{2}\sqrt{2}a$  in the  $y$  direction.

#### D. Mechanisms of diatomic-cluster migration and the pair interaction

A valid mechanism of diatomic-cluster migration must be able to explain the observed elementary displacement steps and their relative frequencies of occurrence. Recently considered in some detail are various possible mechanisms of diatomic-cluster migration.<sup>2</sup> A mechanism involving a simultaneous jump of the two atoms has been ruled out since it cannot satisfactorily explain the frequently observed bond-orientation changes. Mechanisms based on a single atomic jump in the [001] direction and based on two uncorrelated atomic jumps in the  $\langle 111 \rangle$ ,  $[1\bar{1}0]$ , and  $[001]$  have been considered.<sup>2</sup> For the purpose of discussing the pair interaction, we will consider briefly here again various possible migration mechanisms.

In Figs. 8(a)–8(c), we show two-jump mechanisms with the atomic jumps along the  $\langle 111 \rangle$ . Three intermediate bond directions,  $[1\bar{1}0]$ ,  $[001]$ , and  $[1\bar{1}\bar{1}]$  are formed by a jump of either of the two atoms in a cluster of bond orientation along the  $[111]$ . Another jump of either of the two atoms along the  $\langle 111 \rangle$  surface channels will return the cluster from its stretched intermediate bond to its original closely packed bond. In Figs. 8(d) and 8(e), the atom jumps over the apex of a surface

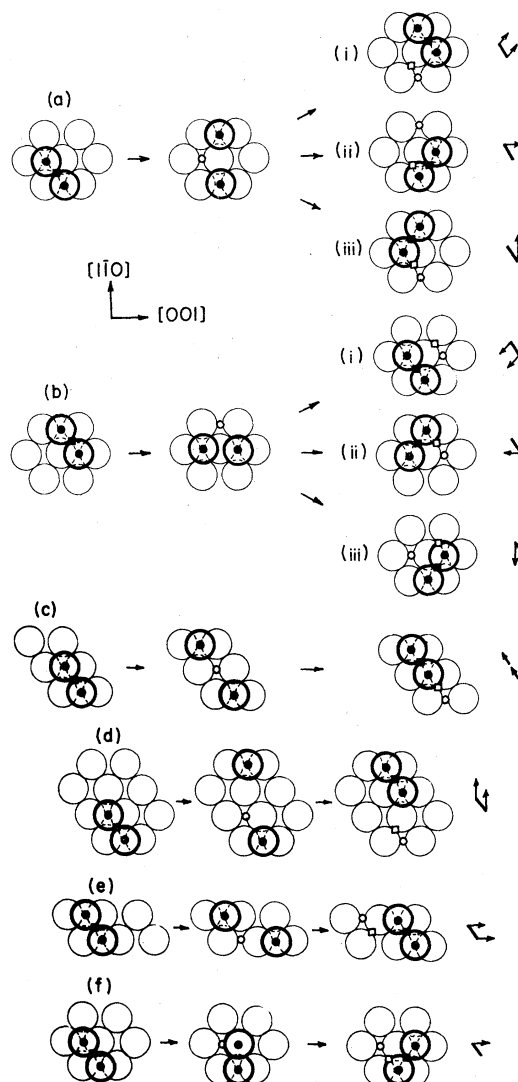


FIG. 8. Mechanisms of the diatomic-cluster migration. For detailed explanation, see the text.

atom in either  $[1\bar{1}0]$  or  $[001]$  direction. In Fig. 8(f), the cluster c.m. displaces by only one atomic jump along the  $[001]$  direction. Symbols of the displacements resulting from these mechanisms are also shown in the figures. Although our experimental data tend to show that all these mechanisms may be occurring to a certain extent as discussed in Sec. II B, we also conclude that  $\alpha$ ,  $\beta$ , and  $\gamma$  steps are the dominant elementary displacement steps. These steps can only be achieved by mechanisms of Figs. 8(a), 8(b), and 8(f). If we denote the rate of transition via two-jump mechanisms with  $[001]$  intermediate-bond state by  $k_1$ , via  $[1\bar{1}0]$  intermediate-bond state by  $k_2$ , and via one-jump mechanism along  $[001]$  by  $k_3$ , then the rates of occurrence of  $\alpha$ ,  $\beta$ , and  $\gamma$  steps are given by

$$\begin{aligned} k_\alpha &= \frac{1}{4}(k_1 + k_2) + k_3, \\ k_\beta &= \frac{1}{4}(k_1 + k_2), \\ k_\gamma &= \frac{1}{4}(k_1 + k_2). \end{aligned} \quad (25)$$

The factor  $\frac{1}{4}$  accounts for the fact that two atomic jumps can also return the cluster to its original position without a net displacement. The anisotropy factor of diatomic migration as defined by Eq. (23) is given by

$$R = 2/[1 + 2k_3/(k_1 + k_2)]. \quad (26)$$

The percentage orientation change is given by

$$(k_\alpha + k_\beta)/(k_\alpha + k_\beta + k_\gamma) = \frac{2}{3}[1 + 2k_3/(k_1 + k_2)]. \quad (27)$$

One can see that exclusively with the three mechanisms, the anisotropy factor of migration can never exceed 2. At 299 K, the experimentally measured value of  $R = 1.70$  is consistent with this mode of migration. However at 309 K,  $R = 2.53$  is obtained. The anisotropy factor is a very sensitive function of the detail mechanisms of diatomic migration. The disagreement indicates that at higher temperatures, nearest-neighbor discrete jump may not be sufficient to describe both the single-atom and diatomic-cluster migrations. Also, the atomic jumps in diatomic-cluster migration may be correlated as discussed in the Appendix, which most definitely shows that the one jump mechanism is less important.

The percentage orientation change as given by Eq. (27) gives a value of 66.7% if one omits the one-jump mechanism along the  $[001]$  direction. This value agrees quite well with the measured values of 68.2% at 299 K and 68.0% at 309 K, indicating that the two-jump mechanisms with the  $[1\bar{1}0]$  and the  $[001]$  intermediate bonds are the dominant mechanisms in the diatomic-cluster migration, although they are not the exclusive ones. Despite our considerable effort of present-

ing data obtained from as many as 1265 heating periods, statistics are only sufficient to consider the  $[1\bar{1}0]$  and  $[001]$  intermediate bonds two-jump mechanisms quantitatively; we will simply assume that these two mechanisms are the only mechanisms in the diatomic-cluster migration.

The rates  $k_1$  and  $k_2$  depend on the pair interaction between the two atoms on the surface. Consider first the  $[1\bar{1}0]$  intermediate-bond two-jump mechanism. Since no intermediate bond of the cluster has ever been observed directly in the 1265 heating periods of 60 sec each, we must conclude that the rate-limiting factor in the cluster migration comes from the first atomic jump. The rate of such jump is given by

$$k_2 = \frac{1}{2}\nu_s \exp\left(-\frac{u(\vec{r}_{110}) - u(\vec{r}_0)}{kT}\right), \quad (28)$$

where  $\nu_s$  is the frequency factor for atomic jumps along the  $\langle 111 \rangle$  surface channels,  $u(\vec{r}_0)$  is the potential energy of the cluster at an equilibrium bond separation  $\vec{r}_0$ , and  $u(\vec{r}_{110})$  is the potential energy at the saddle point along the jumping path as shown in Fig. 9. The factor  $\frac{1}{2}$  accounts for the fact that there are four  $\langle 111 \rangle$  directions, thus the jump frequency in a given direction is  $\frac{1}{4}\nu_s$ , but either of the two atoms in the cluster can jump. The potential energies of the cluster at  $\vec{r}_0$  and  $\vec{r}_{110}$  are the sums of the pair interaction energy  $E_c(\vec{r})$  and the surface potential energy for single atoms  $E_s(\vec{r})$  at  $\vec{r}_0$  and  $\vec{r}_{110}$ .

$$u(\vec{r}_0) = E_c(\vec{r}_0) + E_s(\vec{r}_0), \quad (29)$$

$$u(\vec{r}_{110}) = E_c(\vec{r}_{110}) + E_s(\vec{r}_{110}). \quad (30)$$

But

$$E_s(\vec{r}_{110}) - E_s(\vec{r}_0) = E_d \quad (31)$$

by the definition of the activation energy  $E_d$  of the single-atom migration. We have assumed that the saddle point of activation in the single-atom and diatomic-cluster migration is the same, thus

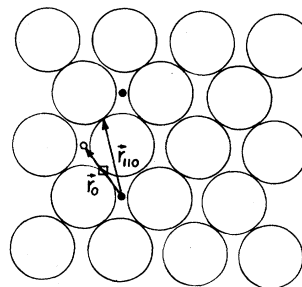


FIG. 9. Diagram showing the bond change during an atomic jump for the two-jump mechanism with an  $[1\bar{1}0]$  intermediate bond direction.

$$k_2 = \frac{1}{2}\nu_s \exp\left(-\frac{E_d + E_c(\vec{r}_{110}) - E_c(\vec{r}_0)}{kT}\right). \quad (32)$$

The rate of atomic jumps for a single atom at the same temperature is given by

$$k_s = \nu_s \exp(-E_d/kT). \quad (33)$$

Thus

$$E_c(\vec{r}_{110}) - E_c(\vec{r}_0) = kT \ln(k_s/2k_2). \quad (34)$$

A similar expression can be written for  $E_c(\vec{r}_{001})$ :

$$E_c(\vec{r}_{001}) - E_c(\vec{r}_0) = kT \ln(k_s/2k_1),$$

where  $\vec{r}_{001}$  is the bond vector at the saddle point along the jumping path of the atom in the two-jump mechanism with a [001] intermediate bond. Neither  $\vec{r}_{110}$  nor  $\vec{r}_{001}$  is precisely known. One may assume that the saddle points are located at the bridge sites along the jumping paths. Also experimentally we do not directly measure  $k_1$  or  $k_2$ , but rather  $k_\alpha$ ,  $k_\beta$ , and  $k_\gamma$ ; they are related by Eq. (25).

$$(k_1 + k_2) \approx \frac{4}{3}(k_\alpha + k_\beta + k_\gamma), \quad (35)$$

if  $k_3 \ll k_1$  and  $k_3 \ll k_2$ .

The rates  $k_1$  and  $k_2$  can be found experimentally by analyzing in detail the rate of displacement in each subcategory as listed in Table I. This can be understood by examining Fig. 8. For a cluster with a certain bond direction, for example along the  $\xi$  axis, the displacement produced by a two-jump mechanism with a  $[1\bar{1}0]$  intermediate-bond direction always points in the opposite direction to the displacement produced by a two-jump mechanism with a [001] intermediate-bond direction. In our detailed analysis of the elementary displacement steps, we did not notice any statistically significant trend. Thus  $k_1$  is nearly equal to  $k_2$  within the limited statistics of the experimental data available. For our discussion, we will simply assume that  $k_1 \approx k_2$ , or  $E_c(\vec{r}_{110}) \approx E_c(\vec{r}_{001})$ . Thus  $k_1 \approx k_2 \approx \frac{2}{3}(k_\alpha + k_\beta + k_\gamma)$ , and

$$\Delta E \equiv E_c(\vec{r}_{\text{sad}}) - E_c(\vec{r}_0) = kT \ln \frac{3k_s}{4(k_\alpha + k_\beta + k_\gamma)}, \quad (36)$$

where  $\vec{r}_{\text{sad}}$  represents either  $\vec{r}_{110}$  or  $\vec{r}_{001}$ .

At 299 K,  $k_s = \bar{N}/\tau = 0.763/60 \text{ sec}^{-1}$  as discussed in Sec. III C. ( $k_\alpha + k_\beta + k_\gamma$ ), the rate of occurrence of  $\alpha$ ,  $\beta$ , and  $\gamma$  steps, can be derived from best fits of the experimental and theoretical two-dimensional displacement distributions as discussed in the Appendix. Direct use of the rates of observation of  $\alpha$ ,  $\beta$ , and  $\gamma$  steps as listed in Table I is invalid as has been discussed earlier. Thus  $(k_\alpha + k_\beta + k_\gamma) \approx (0.19 + 0.15 + 0.145)/60 \text{ sec}^{-1}$ . We have

$\Delta E = E_c(\vec{r}_{110} \text{ or } \vec{r}_{001}) - E_c(\vec{r}_0) = 0.005 \text{ eV}$ . At 309 K,  $k_s = 4.064/60 \text{ sec}^{-1}$ , and  $(k_\alpha + k_\beta + k_\gamma) \approx (0.47 + 0.55 + 0.35)/60 \text{ sec}^{-1}$ . And  $\Delta E = 0.24 \text{ eV}$  is obtained.

Obviously the analysis involved approximations, and the data contains large statistical fluctuations. However, we can conclude that  $\Delta E \approx 0.015 \pm 0.010 \text{ eV}$ . The difference in the interaction between two W atoms on the W {110} plane at  $\sim 2.74 \text{ \AA}$  and at  $\vec{r}_{\text{sad}}$ , which is somewhere between 2.74 and 4.47  $\text{\AA}$ , is very small. This value of  $\Delta E$  is of the same order of magnitude as the difference in the activation energies of diatomic-cluster diffusion and single-atom diffusion,<sup>6</sup> which is  $\sim 0.02 \text{ eV}$ . This is, of course, what is to be expected if the diatomic-cluster migration is accomplished by a bond stretching mechanism, as has been discussed. The fact that the [001] intermediate bond mechanism is not dominant over the  $[1\bar{1}0]$  intermediate bond mechanism suggests that  $u(\vec{r})$  is quite flat over the range from  $\sim 3$  to  $\sim 4.47 \text{ \AA}$ .

The interaction energy at  $\vec{r}_0$ , the closest equilibrium bond separation, for two W atoms on the W {110} plane has been estimated by Tsong<sup>5</sup> to be 0.26 eV and by Bassett and Tice<sup>12</sup> to be 0.31 eV based on dissociation rates observed near 400 K. These results can be summarized as follows:

$$E_c(\vec{r}_0) = -(0.285 \pm 0.018) \text{ eV},$$

$$E_c(\vec{r}_{001} \text{ or } \vec{r}_{110}) = -(0.270 \pm 0.018) \text{ eV}.$$

We must recognize here that the statistical uncertainty is large. Also  $E_c(\vec{r})$  is obtained at only two separations. Only when the amount of data is increased by at least a factor of 10 to 100 can the interaction at larger distances be derived by the rates of occurrence of the other displacement steps observed, but the data were omitted from consideration in this study because of their small numbers. Also, only then can we tell the difference between  $E_c(\vec{r}_{110})$  and  $E_c(\vec{r}_{001})$ .

#### E. Summary

The migration behaviors of single W atoms and W diatomic clusters on the W {110} plane have been investigated by utilizing the atomic resolution capability of the field ion microscope. Although detailed atomic jumps of the migrations cannot be directly seen, they can be studied by measuring the two-dimensional displacement distributions and by the identification of the diatomic-cluster elementary displacement steps. We conclude from these measurements that single W atoms migrate at low temperatures by nearest-neighbor jumps along the  $\langle 111 \rangle$  surface channels. For the diatomic clusters, migration is achieved mainly through three elementary displacement steps. Each of these steps can be produced by two atomic

jumps of the cluster atoms. These atomic jumps are slightly correlated. A correlation factor is defined and derived from least-squares fits of the experimental and calculated two-dimensional displacement distributions. An anisotropy factor of the two-dimensional migration is defined, and experimental data obtained. The pair interaction between two W atoms at the equilibrium separation and at the saddle point of atomic jumps is derived from the frequencies of atomic jumps in single-atom and diatomic-cluster migrations. These frequencies are derived by least-squares fits of the experimental and calculated two-dimensional displacement distribution for both the single atoms and the diatomic clusters. To derive interaction at larger separations, the amount of data needed is formidably large. Only when a better data collection technique is developed, such measurement can become practical. Laser heating of the emitter surface may be an attractive technique for this purpose. This technique will also enable us to study the diffusion behaviors of single atoms and simple atomic clusters at a much higher temperature. At the present time, a molecular dynamic computer simulation of surface diffusion of single atoms and atomic clusters can only be done at a much higher temperature<sup>13</sup> than those accessible to FIM measurements. With a laser heating, the gap can be bridged. A significant progress in understanding the diffusion behaviors can be expected when a direct comparison can be made of the two kinds of studies.

#### ACKNOWLEDGMENTS

This work was supported by NSF Grant No. DMR-7904862. R. C. acknowledges the support of a fellowship from the Universidad de los Andes, Marida, Venezuela.

#### APPENDIX: TWO-DIMENSIONAL DISPLACEMENT DISTRIBUTION FOR DIATOMIC-CLUSTER MIGRATION ON THE W {110}: CENTER-OF-MASS DISPLACEMENTS

In Sec. III B we have discussed a successful identification of three elementary displacement steps:  $\alpha$ ,  $\beta$ , and  $\gamma$  steps. We present here a method for calculating the two-dimensional displacement distribution based solely on the occurrence of  $\alpha$ ,  $\beta$ , and  $\gamma$  elementary displacement steps. Using this method, values of the average numbers of occurrence of the  $\alpha$ ,  $\beta$ , and  $\gamma$  steps within a heating period can be derived by the best fits of the theoretical and experimental displacement distributions. We also show that from these numbers we can conclude that the atomic jumps in the diatomic-cluster migration is slightly cor-

related at the temperatures of our measurements.

As pointed out earlier, the displacement vectors of the center of mass of a diatomic cluster forms a two-dimensional rectangular lattice of  $a\hat{i}/2 \times \sqrt{2}a\hat{j}/2$ . An  $\alpha$ ,  $\beta$ , and  $\gamma$  step produces, respectively, a center-of-mass displacement of  $\pm a\hat{i}/2$ ,  $\pm \sqrt{2}a\hat{j}/2$ , and  $\pm a\hat{i}/2 \pm \sqrt{2}a\hat{j}/2$ . Any one of the lattice points can be reached by a combination of certain numbers of any two of the three elementary steps. We calculate displacement distributions for all possible combinations, and then sum them together by including proper statistical weights. Specifically, the probability of reaching a point  $(x, y)$  starting from  $(0, 0)$  after the occurrence of  $n_\alpha$ ,  $n_\beta$ , and  $n_\gamma$  steps  $W(x, y)$  is given by

$$W(x, y) = p_{\alpha, \beta} W(\alpha, \beta) + p_{\alpha, \gamma_1} W(\alpha, \gamma_1) + p_{\alpha, \gamma_2} W(\alpha, \gamma_2) + p_{\beta, \gamma_1} W(\beta, \gamma_1) + p_{\beta, \gamma_2} W(\beta, \gamma_2), \quad (A1)$$

where  $W(\alpha, \beta)$  represents the probability of reaching the same lattice point, but now is represented by the coordinates  $(\alpha, \beta)$  after the occurrence of  $n_\alpha$ ,  $n_\beta$  of the  $\alpha$  and  $\beta$  steps, and vice versa, and  $p_{\alpha, \beta}$  represents the probability of having this mode of migration, a combination of  $\alpha$  and  $\beta$  steps, and vice versa. The reason for dividing  $\gamma$  into  $\gamma_1$  and  $\gamma_2$  is that for a certain diatomic-cluster orientation, the cluster can only displace in a certain direction by a  $\gamma$  step. For example, a cluster with its bond along the  $\xi$  direction can only displace by a  $\gamma$  step along the  $\zeta$  direction. No such restriction exists for displacing along the  $x$  axis by the  $\alpha$  steps, or along the  $y$  axis by the  $\beta$  steps. The probabilities of having various modes of migration are given by

$$p_{\alpha, \beta} = \frac{n_\alpha n_\beta}{n_\alpha n_\beta + n_\alpha n_\gamma + n_\beta n_\gamma}, \quad (A2)$$

$$p_{\alpha, \gamma_1} = p_{\alpha, \gamma_2} = \frac{1}{2} \frac{n_\alpha n_\gamma}{n_\alpha n_\beta + n_\alpha n_\gamma + n_\beta n_\gamma}, \quad (A3)$$

$$p_{\beta, \gamma_1} = p_{\beta, \gamma_2} = \frac{1}{2} \frac{n_\beta n_\gamma}{n_\alpha n_\beta + n_\alpha n_\gamma + n_\beta n_\gamma}. \quad (A4)$$

$n_\alpha$ ,  $n_\beta$ , and  $n_\gamma$  represent, respectively, the average numbers of occurrences of the  $\alpha$ ,  $\beta$ , and  $\gamma$  steps in a heating period. These numbers are different from the average numbers of observing the  $\alpha$ ,  $\beta$ , and  $\gamma$  steps in a heating period.

A lattice site represented by  $(x, y)$  in the  $x$ - $y$  coordinates is represented, respectively, in the  $\alpha$ - $\beta$ , the  $\alpha$ - $\gamma_1$ , the  $\alpha$ - $\gamma_2$ , the  $\beta$ - $\gamma_1$ , and the  $\beta$ - $\gamma_2$  coordinate systems by  $(\alpha, \beta)$ ,  $(\alpha, \gamma_1)$ ,  $(\alpha, \gamma_2)$ ,  $(\beta, \gamma_1)$ , and  $(\beta, \gamma_2)$ . Figure 10 illustrates this point with an example. In Table VII, lattice points with an  $x$  and  $y$  smaller than or equal to 3 are listed.

The problem is reduced to finding a set of num-



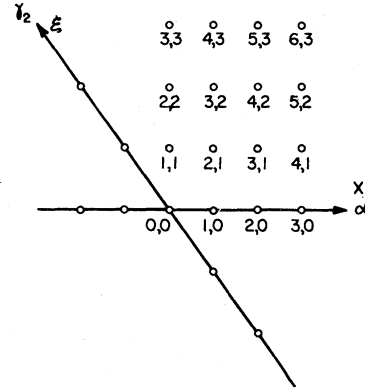
TABLE VII. Coordinates for some sites.

$(x, y)$	$(\alpha, \beta)$	$(\alpha, \gamma_1)$	$(\alpha, \gamma_2)$	$(\beta, \gamma_1)$	$(\beta, \gamma_2)$
0, 0	0, 0	0, 0	0, 0	0, 0	0, 0
1, 0	1, 0	1, 0	1, 0	-1, 1	1, -1
2, 0	2, 0	2, 0	2, 0	-2, 2	2, -2
3, 0	3, 0	3, 0	3, 0	-3, 3	3, -3
0, 1	0, 1	-1, 1	1, 1	1, 0	1, 0
1, 1	1, 1	0, 1	2, 1	0, 1	2, -1
2, 1	2, 1	1, 1	3, 1	-1, 2	3, -2
3, 1	3, 1	2, 1	4, 1	-2, 3	4, -3
0, 2	0, 2	-2, 2	2, 2	2, 0	2, 0
1, 2	1, 2	-1, 2	3, 2	1, 1	3, -1
2, 2	2, 2	0, 2	4, 2	0, 2	4, -2
3, 2	3, 2	1, 2	5, 2	-1, 3	5, -3
0, 3	0, 3	-3, 3	3, 3	3, 0	3, 0
1, 3	1, 3	-2, 3	4, 3	2, 1	4, -1
2, 3	2, 3	-1, 3	5, 3	1, 2	5, -2
3, 3	3, 3	0, 3	6, 3	0, 3	6, -3

bers for  $n_\alpha$ ,  $n_\beta$ , and  $n_\gamma$  which give a best fit by least squares with the experimentally measured two-dimensional displacement distributions listed in Figs. 5(a) and 5(b) as the upper numbers. In Table VIII, the best fit set of calculated values are listed. The 299 K data fits best with  $n_\alpha = 0.190 \pm 0.005$ ,  $n_\beta = 0.150 \pm 0.005$ ,  $n_\gamma = 0.145 \pm 0.005$ . The 309 K data fits best with  $n_\alpha = 0.47 \pm 0.01$ ,  $n_\beta = 0.55 \pm 0.01$ , and  $n_\gamma = 0.35 \pm 0.01$ . All these values are in a unit of  $(\text{min})^{-1}$ .

As can be seen from Table VIII, the best fit sets of calculated values agree with experimental values very well over all sites. Thus at least at low temperatures, below about 310 K, the migration behavior of W diatomic clusters can be adequately accounted for by the  $\alpha$ ,  $\beta$ , and  $\gamma$  elementary steps. Some of the other observed displacements may also be elementary, but the rate of occurrence is too small to be established without any doubt with the amount of data now available.

It is noted that the numbers of  $\gamma$  steps at both 299 and 309 K are significantly lower than the

FIG. 10. Coordinates of some sites in  $x$ - $y$  and  $\alpha$ - $\gamma_2$  coordinate systems.

numbers of  $\alpha$  and  $\beta$  steps. If an elementary displacement step is achieved by two uncorrelated atomic jumps, then  $n_\gamma$  should be equal to  $(n_\alpha + n_\beta)/2$ , irrespective of whether or not the jumps with an  $[1\bar{1}0]$  intermediate bond is favored more than the jumps with a  $[001]$  intermediate bond. The fact that the  $\gamma$ -step occurs less frequently than  $(n_\alpha + n_\beta)/2$  indicates quite clearly that the two atomic jumps are slightly correlated. It can be easily understood with the help of Fig. 2 that, if an atom which starts the first jump also makes the second jumps, then only the  $\alpha$ -step and the  $\beta$ -step can be observed. Let us assume that a fraction  $f$  of the atomic jumps are correlated, namely, two successive jumps by the same atom, then

$$n_\alpha = [\frac{1}{3}(1-f) + \frac{1}{2}f]C, \quad (\text{A5})$$

$$n_\beta = [\frac{1}{3}(1-f) + \frac{1}{2}f]C, \quad (\text{A6})$$

$$n_\gamma = \frac{1}{3}(1-f)C, \quad (\text{A7})$$

where  $C$  is a proportionality constant obviously given by

$$C = n_\alpha + n_\beta + n_\gamma. \quad (\text{A8})$$

Thus

TABLE VIII. Two-dimensional displacement distributions.

$x, y$	299 K		309 K	
	Expt. $W(x, y)$ (%)	Calc. $W(x, y)$ (%)	Expt. $W(x, y)$ (%)	Calc. $W(x, y)$ (%)
0, 0	73.32	73.20	44.33	44.15
1, 0	4.99	5.05	7.75	7.52
2, 0	0.26	0.23	0.70	0.81
0, 1	3.75	3.73	9.05	8.81
1, 1	1.94	1.88	3.23	3.44
0, 2	0.20	0.13	1.49	1.14
All	1.97	1.00	8.57	5.53
others				

$$f = 1 - \frac{3n_\gamma}{(n_\alpha + n_\beta + n_\gamma)}. \quad (\text{A9})$$

This fraction may be called a "correlation factor" for atomic jumps in the diatomic-cluster migration and can therefore be easily calculated. Using the values of  $n_\alpha$ ,  $n_\beta$ , and  $n_\gamma$  derived, we find that  $f(299 \text{ K}) = 0.10$ , and  $f(309 \text{ K}) = 0.23$ . The fact that the correlation factor is larger at higher temperature is in fact consistent with a molecular dynamics computer simulation of surface diffusion in which Tully *et al.*<sup>13</sup> find that at higher temperatures atoms tend to jump not to a nearest neighbor site, but over several atomic distances. It is also consistent with a single W atom diffusion experiment on the W {110} plane carried out at 330

K, where an experimental two-dimensional displacement distribution fits best with an exponential jump length distribution given by<sup>10</sup>

$$p(jl) = C \exp(-\alpha j), \quad (\text{A10})$$

where  $j$  is an integer other than 0,  $l$  is the nearest-neighbor distance, and  $C$  is a constant given by

$$C = \frac{1}{2} [\exp(\alpha) - 1], \quad (\text{A11})$$

where  $\alpha = 2.04 \pm 0.16$ . This result indicates that at 330 K, about  $(13 \pm 2)\%$  of the atomic jumps in single-atom W diffusion on the W {110} plane goes beyond the first nearest-neighbor distance.

<sup>1</sup>See, for example, E. W. Muller and T. T. Tsong, *Field Ion Microscopy, Principles and Applications* (American Elsevier, New York, 1969).

<sup>2</sup>T. T. Tsong and R. Casanova, *Phys. Rev. B* **21**, 4564 (1980).

<sup>3</sup>T. T. Tsong, *Phys. Rev. B* **7**, 4018 (1973).

<sup>4</sup>G. Ehrlich and F. G. Hudda, *J. Chem. Phys.* **44**, 1039 (1966); G. Ayrault and G. Ehrlich, *ibid.* **60**, 281 (1974).

<sup>5</sup>T. T. Tsong, *Phys. Rev. B* **6**, 417 (1972).

<sup>6</sup>P. L. Cowan and T. T. Tsong, *Phys. Lett. A* **53**, 383 (1975).

<sup>7</sup>D. W. Bassett and P. J. Parshly, *Nature (London)* **221**, 1046 (1969).

<sup>8</sup>G. Ehrlich, *J. Chem. Phys.* **44**, 1050 (1966).

<sup>9</sup>K. Lakatos-Lindenberg and K. E. Shuler, *J. Math. Phys.* **12**, 633 (1971).

<sup>10</sup>P. L. Cowan and T. T. Tsong (unpublished).

<sup>11</sup>G. L. Kellogg and T. T. Tsong, *J. Appl. Phys.* **51**, 1184 (1980).

<sup>12</sup>D. W. Bassett and D. R. Tice, *Surf. Sci.* **40**, 499 (1973).

<sup>13</sup>J. C. Tully, G. H. Gilmer, and M. Shugard, *J. Chem. Phys.* **71**, 1630 (1979).

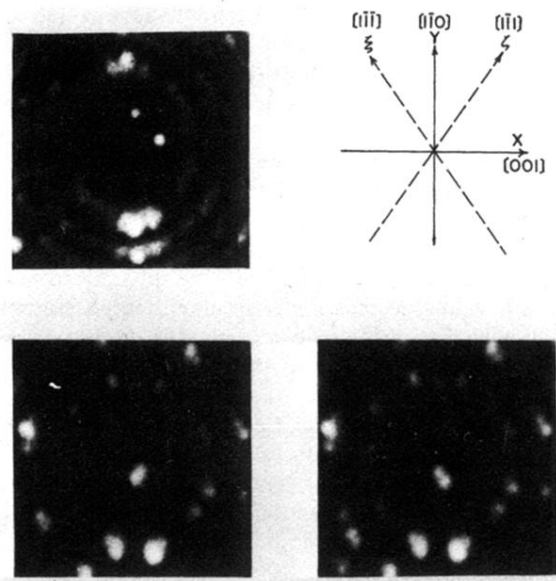


FIG. 1. Field ion images showing two W atoms on a W  $\{110\}$ , a W diatomic cluster oriented along the  $[1\bar{1}1]$ , and one oriented along the  $[1\bar{1}\bar{1}]$ .